

Laminin Receptor Involvement in the Anti-angiogenic Activity of Pigment Epithelium-derived Factor^{*,§,♦}

Received for publication, December 9, 2008, and in revised form, February 11, 2009 Published, JBC Papers in Press, February 17, 2009, DOI 10.1074/jbc.M809259200

Adrien Bernard[‡], Jacqueline Gao-Li[‡], Claudio-Areias Franco[‡], Tahar Bouceba[§], Alexis Huet[¶], and Zhenlin Li^{‡,1}

From the [‡]Université Pierre et Marie Curie, Université Paris 06, UR4, Aging, Stress and Inflammation and [§]Institut Fédératif de Recherche 83, 75252 Paris, France and the [¶]Université Paris-Sud XI, CNRS Unité Mixte de Recherche 8619, IBBMC, 91400 Orsay, France

Pigment epithelium-derived factor (PEDF) is a multifunctional protein with neurotrophic, anti-oxidative, and anti-inflammatory properties. It is also one of the most potent endogenous inhibitors of angiogenesis, playing an important role in restricting tumor growth, invasion, and metastasis. Studies show that PEDF binds to cell surface proteins, but little is known about how it exerts its effects. Recently, research identified phospholipase A₂/nutrin/patatin-like phospholipase domain-containing 2 as one PEDF receptor. To identify other receptors, we performed yeast two-hybrid screening using PEDF as bait and discovered that the non-integrin 37/67-kDa laminin receptor (LR) is another PEDF receptor. Co-immunoprecipitation, His tag pulldown, and surface plasmon resonance assays confirmed the interaction between PEDF and LR. Using the yeast two-hybrid method, we further restricted the LR-interacting domain on PEDF to a 34-amino acid (aa) peptide (aa 44–77) and the PEDF-interacting domain on LR to a 91-aa fragment (aa 120–210). A 25-mer peptide named P46 (aa 46–70), derived from 34-mer, interacts with LR in surface plasmon resonance assays and binds to endothelial cell (EC) membranes. This peptide induces EC apoptosis and inhibits EC migration, tube-like network formation *in vitro*, and retinal angiogenesis *ex vivo*, like PEDF. Our results suggest that LR is a real PEDF receptor that mediates PEDF angiogenesis inhibition.

Pigmented epithelium-derived factor (PEDF)^{,2} also known as SERPIN F1 and EPC1, is a 50-kDa serpin-like peptide. Although

first identified in cultured pigment epithelial cells from fetal human retinas (1), we now know that liver, kidney, heart, testis, and lung tissues also express PEDF (2). PEDF influences many biological processes. It is anti-angiogenic, anti-tumorigenic, anti-inflammatory, anti-oxidative, neurotrophic, and neuro-protective, and it exhibits anti-vasopermeability properties (3–9). These diverse actions affect many cell types, including retinal cells (10), neuronal cells (11), endothelial cells (12), and hematopoietic stem cells (13). X-ray diffraction studies show that PEDF has an asymmetrical charge distribution (14). A high density of basic residues on one side of the molecule (positive) interact with heparin and glycosaminoglycans, whereas acidic residues on the opposite side (negative) interact with type-1 collagen (15–19). Yet the mechanisms explaining the diverse biological activities of PEDF remain unclear.

A ligand/receptor interaction at the cell membrane seemed likely, in addition to interactions within extracellular matrices, because of the diverse effects and ubiquitous expression of PEDF and the fact that most PEDF deposits remain within extracellular matrices (20). We suspected that distinct PEDF receptors elicit divergent signals to cause different biological effects. Indeed, evidence shows that PEDF binds at least two receptors: a 60-kDa receptor in ECs and an 80-kDa receptor in neuronal cells (21–24). Research has identified two functional epitopes on PEDF: a 34-mer peptide (residues 44–77) and a 44-mer peptide (residues 78–121) (25). The 44-mer peptide interacts with the putative 80-kDa receptor identified on Y-79 cells and cerebellar, motor (21, 22), and retinal (23) neurons, to replicate the neurotrophic and anti-vasopermeability properties of PEDF (9, 25). Becerra and co-workers (26) recently identified 80-kDa PLA2/nutrin/patatin-like phospholipase domain-containing 2 (PNPLA2) as a PEDF receptor that binds the 44-mer epitope. Filleur *et al.* (25) showed *in vivo* that overexpressing the 34-mer in PC-3 prostate adenocarcinoma cell lines reduces tumor microvessel density and increases apoptosis. The 34-mer peptide induces apoptosis, blocks endothelial cell migration, and inhibits corneal angiogenesis, possibly through a distinct EC receptor. We do not yet know the nature of the 60-kDa receptor.

PEDF is one of the most potent natural endogenous inhibitors of angiogenesis, the extension of the vascular network from pre-existing blood vessels. It inhibits endothelial cell migration even in the presence of pro-angiogenic factors, such as vascular

hemagglutinin; EC, endothelial cell; X-α-Gal, 5'-bromo-4-chloro-3'-indolyl-α-D-galactopyranoside.

* This work was supported by funds from the Association pour la Recherche sur le Cancer (ARC, 3587, to Z. L.) and by fellowships from ARC and Naturalia et Biological (to A. B.), Retina France (to J. G.), and Fondation de Recherche Médicale (to C. A. F.).

♦ This article was selected as a Paper of the Week.

§ The on-line version of this article (available at <http://www.jbc.org>) contains supplemental Fig. S1 and S2.

¹ To whom correspondence should be addressed: Université Pierre et Marie Curie, UR4, Aging, Stress and Inflammation, BP256, 7 Quai St-Bernard, 75005 Paris, France. Tel.: 33-1-44-27-21-36; Fax: 33-1-44-27-21-35; E-mail: zhenlin.li@upmc.fr.

² The abbreviations used are: PEDF, pigment epithelium-derived factor; AD, activation domain; BD, binding domain; KAP, keratin-associated protein; LR, laminin receptor; PNPLA2, PLA2/nutrin/patatin-like phospholipase domain-containing 2; RU, resonance unit; TUNEL, terminal deoxynucleotidyl transferase-mediated biotin-dUTP nick end labeling; Y2H, yeast two-hybrid; aa, amino acid(s); HuBMEC, human bone marrow endothelial cell; VEGF, vascular endothelial growth factor; bFGF, basic fibroblast growth factor; MAPK, mitogen-activated protein kinase; JNK, c-Jun N-terminal kinase; FBS, fetal bovine serum; Ni-NTA, nickel-nitrilotriacetic acid; PBS, phosphate-buffered saline; DAPI, 4',6'-diamino-2-phenylindole; SPR, surface plasmon resonance; siRNA, small interfering RNA; HA,

endothelial growth factor (VEGF) and fibroblast growth factor (FGF) (27–29). PEDF-deficient mice show increased stromal microvessel density in several organs, such as the pancreas and prostate, suggesting that PEDF plays a key role as a natural angiogenesis inhibitor (30). PEDF activity is selective. It only targets new vessel growth and spares pre-existing vasculature. It seems that the anti-angiogenic effects of PEDF involve endothelial cell death through the activation of the Fas/FasL death pathway (31). MAPK JNK and p38 influence endothelial cell apoptosis by modulating c-FLIP or caspase activity in the presence of PEDF (32, 33). Recently, Cai *et al.* (34) reported that PEDF inhibits VEGF-induced angiogenesis in retinal ECs. PEDF enhances γ -secretase-dependent cleavage of the C terminus of VEGF receptor-1, thus blocking VEGF receptor-2 induced angiogenesis.

This study aimed to investigate potential receptors for PEDF and to establish how they influence angiogenesis. We used a yeast two-hybrid (Y2H) approach to identify potential PEDF partners, paying particular attention to proteins that could be PEDF receptors. Our results demonstrate that the non-integrin 37/67-kDa laminin receptor (LR) is a new PEDF receptor. LR could be the proposed 60-kDa receptor identified in ECs (24). LR is not simply a laminin receptor. It also mediates prion protein internalization (35) and functions as a receptor for viruses, such as Sindbis, dengue, and adeno-associated virus (36–38). The LR subunit is implicated in several physiological and pathological processes, including cell differentiation, growth, migration, and cancer invasion (39). Our research shows that LR helps mediate PEDF anti-angiogenic activities. We identified both a 25-mer LR-interacting domain on PEDF and a PEDF-interacting domain on LR. The 25-mer PEDF-derived peptide exerts the same anti-angiogenic and pro-apoptotic effects on ECs as PEDF.

EXPERIMENTAL PROCEDURES

Y2H Screening of PEDF Partners—We used a Matchmaker GAL4 two-hybrid system of *Saccharomyces cerevisiae* AH109 strain (Clontech) to screen a human skeletal muscle Matchmaker cDNA library (Clontech), with their 5' ends proximal to the activation domain (AD) of the GAL4 transcription factor in a pACT2 vector. We used full-length PEDF cDNA (accession number NM_002615) baits, cloned in a pGBKT7 vector, with the GAL4-binding domain (BD) at their 5' end. We performed interaction selection on high stringency medium (SD/–Ade/–His/–Leu/–Trp/X- α -Gal). The AD-containing plasmids in the selected clones were isolated according to the manufacturer's instructions. We determined the cDNA nucleotide sequences in each clone (genome-express, Meylan, France) and compared them with the GenBankTM data base by using the BLAST search program.

Y2H Method to Identify Laminin Receptor and PEDF Interaction—We PCR-amplified different human PEDF fragments (encoding amino acids 2–418, 140–418, 206–418, 374–418, 2–326, 2–140, 2–86, 2–44, 44–121, and 44–77; see Fig. 1) and cloned them into the EcoRI and BamHI sites of the pGBKT7 vector. Similarly, we PCR-amplified LR fragments (encoding amino acids 2–295, 96–295, 96–295del158–179, 120–210, 135–200, 157–210, 120–180, and 157–180) with

probes containing EcoRI and BamHI sites and cloned them into pGADT7. We verified the constructions by sequencing. We studied the potential interaction between different fragments of PEDF and LR by co-transforming them into the *S. cerevisiae* AH109 strain, as described above. Yeast immunofluorescence was performed as described (40) with anti-GAL4-AD and anti-GAL4-BD (Santa Cruz). Yeast protein extracts were carried out as described (41) and analyzed with anti-GAL4-AD and anti-LR (Santa Cruz) in Western blot analysis.

Cell Cultures—Human bone marrow endothelial cells (HuBMEC) (42) were grown in endothelial cell basal medium 2 (Promocell, Heidelberg, Germany). We cultured cells in plates coated with 0.2% gelatin (Sigma) at 37 °C in a humidified atmosphere of 5% CO₂. We grew COS7 cells in Dulbecco's modified Eagle's medium, supplemented with 10% FBS with 100 units/ml penicillin and 100 μ g/ml streptomycin.

Expression Vector Construction and Transfection into Cell Cultures—We cloned full-length PEDF (aa 2–418) and LR (aa 2–295) cDNAs in pCMV-HA and pCMV-Myc vectors (Clontech) to obtain pCMV-HA-tagged-PEDF (HA-PEDF) and Myc-tagged-LR (Myc-LR) expression vectors, respectively. We then co-transfected these two constructions into COS-7 cells that we had plated at 1.5×10^5 cells/well the previous day using Matra transfection reagent, according to the manufacturer's instructions (IBA, Göttingen, Germany).

PEDF Expression in Insect Cells and Laminin Receptor Expression in Escherichia coli—We used the primers PEDF2 (5'-AATGAATTCCAGGCCCTGGTGCTACTCCTC-3') and PEDFR (5'-CCTCTAGACTGGGGCCCCCTGGGGTCCAG-3') to PCR amplify human PEDF cDNA (2–418). We cloned this fragment into the EcoRI and XbaI sites of the pIB/V5-His/CAT vector (Invitrogen). Primers LR2 (5'-ACTGAATTCTCCGAGCCCTTGATGTCCTG-3') and LR reverse primer (5'-ACTGCGGCCGCAGACCAGTCAGTGGTTGCTCC-3') or LR90 (5'-ACTGAATTGCGCACTCCAATTGCTGGCCGC-3') and LRR were used to PCR amplify human LR (2–295) or LR90 (90–295) fragments, respectively. We cloned these fragments into the EcoRI and NotI sites of the pSCodon2 vector (Delphi Genetics, Charleroi, Belgium). We purified PEDF from Sf9 insect cells after blasticidin selection and purified laminin receptor from SE1 bacteria after isopropyl β -D-thiogalactopyranoside induction with Ni-NTA-agarose resin (Qiagen), according to the manufacturer's instructions.

Immunofluorescence—COS-7 cells were co-transfected with HA-PEDF and Myc-LR. Forty-eight hours later, we rinsed them with PBS twice and fixed them in 4% paraformaldehyde for 5 min, followed by 50 mM NH₄Cl for 15 min. We permeabilized cells with PBS containing 0.1% Triton X-100 for 10 min. We then incubated the permeabilized cells with PBS containing 2% bovine serum albumin for 20 min before incubating them with either anti-PEDF antibody (MAB1059, 1:100; Chemicon, Temecula, CA) and anti-LR antibody (H-141, 1:100; Santa Cruz) or anti-HA antibody (3F10, 1:100; Roche Applied Science) and anti-Myc tag antibody (9B11, 1:2000; Cell Signaling, Beverly, MA) in PBS containing 0.2% bovine serum albumin for 1 h. We washed cells four times with PBS and incubated them with Cy3-conjugated Goat anti-rabbit antibody (1:400, Jackson ImmunoResearch; Suffolk, UK) or Alexa Fluor 488 goat anti-

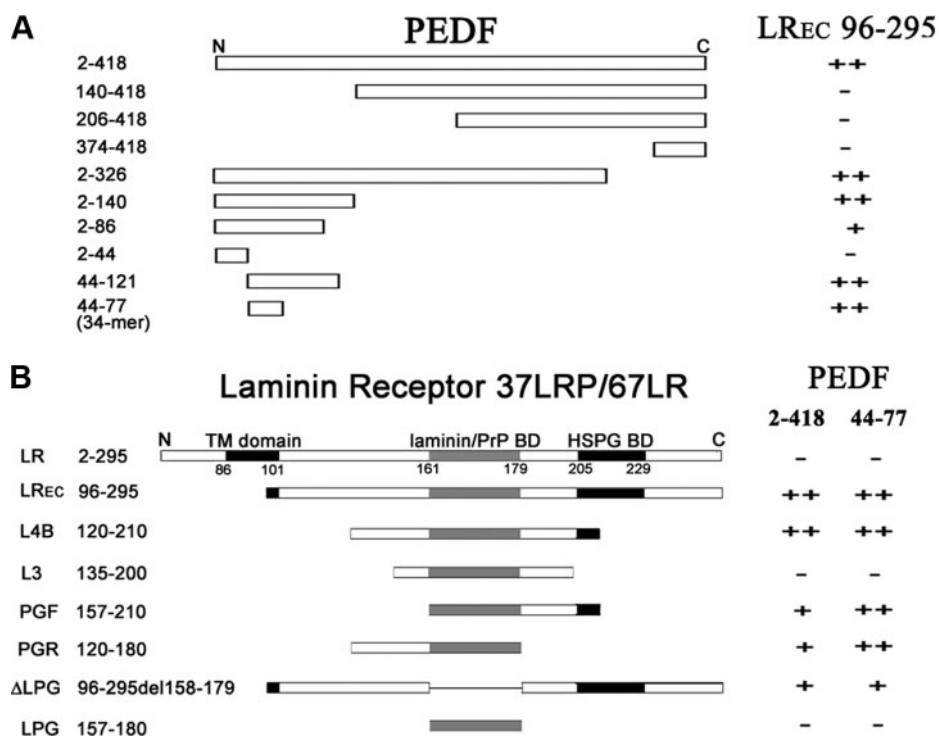


FIGURE 1. Finding PEDF-LR interaction domains by yeast two-hybrid assay. *A*, identifying a direct LR-interacting domain on PEDF. Using full-length PEDF (aa 2–418) as bait, we identified the extracellular domain of LR (LREC 96–295) as a PEDF partner. We designated their interaction level as ++ and compared other experiments to this, labeling them as ++, +, and – depending on the speed of yeast growth and the blue staining of galactosidase activity. The corresponding amino acid numbers in each construct are indicated to the left of the figure. The interaction level is marked to the right of the figure. We identified one LR-interacting domain (aa 44–77) in N terminus. This fragment (aa 44–77) has also been identified as the anti-angiogenic peptide 34-mer (25). *B*, identifying the PEDF-interacting domain on LR. We tested the interactions between different fragment lengths of 67LR and full-length PEDF (2–418) or the 34-mer fragment. The PEDF-interacting domain on LR was localized to the region 120–210. The laminin/prion-binding domain (laminin/PrP BD) or peptide G (aa 157–180) alone was not sufficient for PEDF-LR interaction. However, deleting this region reduces PEDF-LR interaction. TM, transmembrane; HSPG BD, heparan sulfate proteoglycan-binding domain.

mouse IgG (1:400; Molecular Probes, Carlsbad, CA) for 1 h in the dark. We washed the cells three times in PBS before incubating them with DAPI (dilution 1:10000, Sigma) for 5 min. We washed cells twice before mounting them onto glass slides with a drop of Mowiol mounting medium.

Molecular Modeling—We modeled the PEDF-interacting domain using VMD software. We reduced the region into a theoretical functional domain with the help of a server and a docking server simulating an interaction between the peptide and ribosomal protein S2, which shares a 52% sequence homology with LR. One peptide, 25-mer P46 (aa 46–70, FFKVPVNK-LAAVSNFGYDLYRVRS) was determined and synthesized (see Fig. 3). We also synthesized fluoroscein-coupled peptide (F46) (Engineering protein platform, IFR83, UPMC, Paris, France).

Surface Plasmon Resonance (SPR) Assays—Using a BIAcore 3000 instrument (Biacore AB, Uppsala, Sweden), we analyzed the molecular interaction in real time between PEDF or PEDF-derived peptide P46 and his-LR (aa 2–295) or his-LR90 (aa 90–295) isolated from *E. coli* and immobilized on a NTA sensor chip to reach a response of between 1200 and 1600 resonance units (RU), according to the manufacturer's recommendations. We prepared a reference surface, without protein, by the same procedure. To evaluate nonspecific background signals, we also used PEDF protein and peptide P46 on NTA chips

uncoated with His-LR. Running buffer (10 mM HEPES, 150 mM NaCl, 50 μ M EDTA, 0.005% surfactant P20, pH 7.4) and binding buffer (10 mM HEPES, 150 mM NaCl, 5 mM CaCl₂, 50 μ M MgCl₂, 50 μ M EDTA, 0.005% surfactant P20, pH 7.4) were used. We used PEDF protein (reference number 01-211; Upstate) and peptide P46 to study binding. We analyzed results with BIA evaluation software version 4.1.

F46 Binding to Cells—We grew HuBMECs to a 60–80% confluency before incubating them with fluoroscein-coupled-P46 peptide (F46, 50 or 200 nM) at 4 °C for 60 min. To test the binding specificity, we used either nonfluorescent peptide (P46) at 500 μ M or anti-LR antibodies in the binding assay. In the latter case, HuBMECs were first preincubated for 30 min with LR antibody (67LR, ab711, 1:100; Abcam, Cambridge, UK; or LR antibody, H-141, 1:100; Santa Cruz) at 37 °C, followed by placing the plate at 4 °C for 30 min, prior to incubation with F46 (50 or 200 nM) at 4 °C for 1 h. We washed cells three times with PBS and then fixed them with 4% paraformaldehyde for 5 min, incubated them with PBS containing DAPI, then washed,

and mounted them beneath glass coverslips. We took photographs with a Zeiss LSM510 confocal laser microscope (Göttingen, Germany). We used a nonrelevant rhodamin-labeled 25-mer peptide KAP3.1 (FSDKSCRCGVCLPSTCPHEISLLQP) derived from keratin-associated protein (43) as a control peptide.

Western Blot Analysis—We extracted proteins using radio-immune precipitation assay buffer (1 mM EDTA, 1% Triton X-100, 1% sodium deoxycholate, 0.1% SDS, 150 mM NaCl, 50 mM Tris-HCl, pH 7.25, 1 mM phenylmethylsulfonyl fluoride, and a mixture of protease inhibitors (Roche Applied Science)). We determined protein amounts using Bradford reagent (Bio-Rad). We denatured 20 μ g of protein with reducing Laemmli buffer and resolved them with 12% SDS-PAGE. We then transferred the proteins to the polyvinylidene difluoride membranes (Amersham Biosciences). We blocked the membranes with 5% fatty acid-free milk at room temperature for 1 h. We then incubated the membranes overnight at 4 °C, with the primary antibodies (LR antibody, H-141, 1:250; Santa Cruz; and active caspase-3, CPP32, 1:1000; R & D System) diluted in 5% milk, followed by incubation with a secondary antibody conjugated with peroxidase (Dako, Glostrup, Denmark). We used ECL detection reagent to detect signals. The values obtained with ImageJ software were normalized with anti-glyceraldehyde-3-phosphate dehydrogenase antibody (FL-335, 1:400; Santa Cruz).

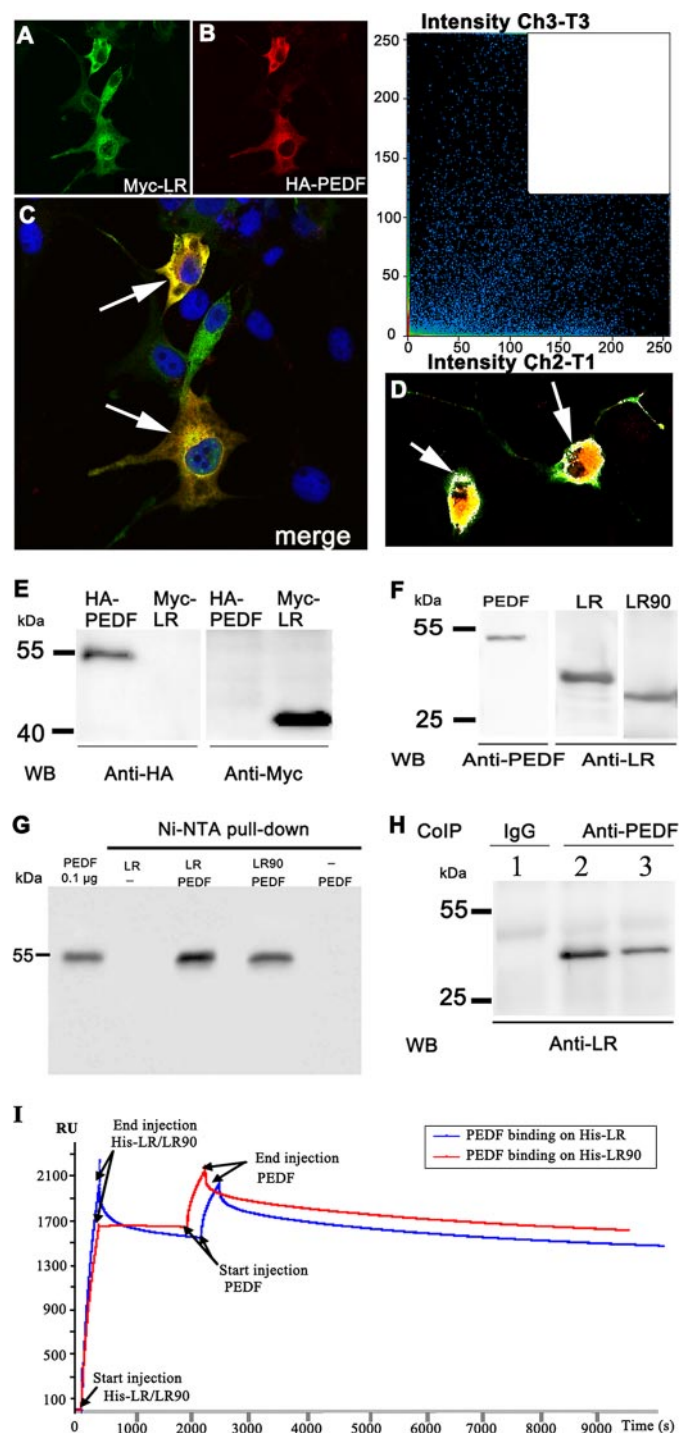


FIGURE 2. Co-localization of HA-PEDF and Myc-LR in cell cultures and PEDF-LR interaction in vitro. *A* and *B*, we immunostained Myc-LR and HA-PEDF co-transfected COS7 cells with anti-Myc antibody (green) and anti-HA antibody (red) 48 h after transfection. *C*, the merged image of *A* and *B* indicates the co-localization of PEDF and LR in the co-transfected cells (arrows). *D*, confocal microscopy image analysis of HA-PEDF and Myc-LR in COS7 cells with the software Coloc. The white color in the plot in the upper right corner corresponds to the co-localization of high density red color (Ch3-T3) and green color (Ch2-T1) (between 120 and 250) staining. This co-localization occurred mainly around the plasma membrane (arrows). *E*, Western blot (WB) analysis of COS7 cells transfected with anti-HA and anti-Myc antibodies. We found HA-PEDF at 55 kDa and Myc-LR at 40 kDa. The plasmids used in transfection are indicated at the top of the picture, and molecular mass markers are to the left. *F*, we confirmed PEDF expression in insect Sf9 cells and LR or LR90 in *E. coli* by Western blot, using anti-PEDF antibody and anti-LR antibody. *G*, PEDF was pulled down with Ni-NTA resin when His-tag LR or His-tag LR90 was

Co-immunoprecipitation—We incubated the protein mixtures at 4 °C for 1 h with 2 µg of anti-PEDF antibody (Chemicon) on a mixing rotor. We added agarose A/G protein (20 µl) and incubated the samples overnight. The next day, we centrifuged the samples at 1000 × *g* for 5 min. We removed the supernatant, leaving a pellet of beads. We washed the pellets four times by centrifuge (1000 × *g*, 5 min) with radioimmune precipitation assay buffer (1 ml) (1× PBS, pH 7.4, 1% Nonidet P-40, 0.5% sodium deoxycholate, 0.1% SDS), adding Laemmli buffer after the last wash. We performed Western blot analysis with anti-LR antibody (H-141, 1:250; Santa Cruz) as described above.

His Tag Pull-down Assay—We assessed PEDF binding to His-tagged LR by His tag pull-down of bound complexes with Ni-NTA resin, as described by Notari *et al.* (26). PEDF protein (2 µg; Upstate) was mixed with either 1 µg of His-LR (aa 2–295) or 1 µg of His-LR90 (aa 90–295, extracellular domain), purified from *E. coli* by Ni-NTA resin (more than 95% purity) in binding buffer (50 mM sodium phosphate, pH 7.5, 500 mM NaCl, 1% Nonidet P-40; final volume, 150 µl), and incubated at 4 °C for 4 h with gentle rotation. We added the Ni-NTA resin beads (50 µl), pre-equilibrated in binding buffer, to the mixture and incubated at 4 °C for 2 h with gentle rotation. Brief centrifugation sedimented the resin beads, and we washed them three times with binding buffer. We extracted the proteins with 50 µl of 2× Laemmli buffer and analyzed them by Western blot with anti-PEDF antibody.

Matrigel Angiogenesis Assay—We performed this assay as previously described (44). HuBMECs were seeded in 24-well plates, precoated with 300 µl of growth factor-reduced Matrigel (BD Bioscience), at 48,000 cells/well. We cultured cells for 24 h in Dulbecco's modified Eagle's medium, supplemented with 0.2% FBS, 100 units/ml penicillin, and 100 µg/ml streptomycin. We examined the effects of PEDF, 25-mer peptide P46, or control peptide KAP3.1 on bFGF-induced tube-like networks by phase contrast microscopy. We took representative photographs from four random fields/sample and measured the endothelial tube lengths. We then performed three distinct experiments.

Corneal Angiogenesis—We assessed corneal angiogenesis as described previously (45). Sucralfat pellets containing PBS alone, bFGF alone, bFGF plus PEDF, bFGF plus peptide P46, or P46 alone were implanted into the corneas of C57/B16 mice. We used about 30 ng of bFGF, 50 ng of PEDF, and 10 ng of P46/pellet. Three to eight animals (6–11 corneal implants) were examined per sample. We used an Olympus SCH10 microscope to examine the eyes of the mice. The Pierre and Marie Curie University Animal Care and Use Committee had approved the protocol.

Apoptosis Assay—We performed terminal deoxynucleotidyl transferase-mediated biotin-dUTP nick end labeling (TUNEL) using an *In Situ* Cell Death Detection Kit (Roche Applied Science). We seeded HuBMECs at 3.8 × 10⁴ cells/well in 24-well

present in the mixture. *H*, co-immunoprecipitation of PEDF and LR. Anti-LR only detected 40 kDa LR when we used anti-PEDF antibody (lanes 2 and 3) in the mixture containing full-length LR and PEDF, but not when we used control IgG (lane 1.). *I*, real time binding by SPR analyses of PEDF and LR interactions. We recorded sensograms with His-LR or His-LR90 immobilized on a NTA sensor Chip and PEDF using a BIAcore 3000 instrument and BIAevaluation software. We observed similar interactions (370 RU) between PEDF and LR or LR90.

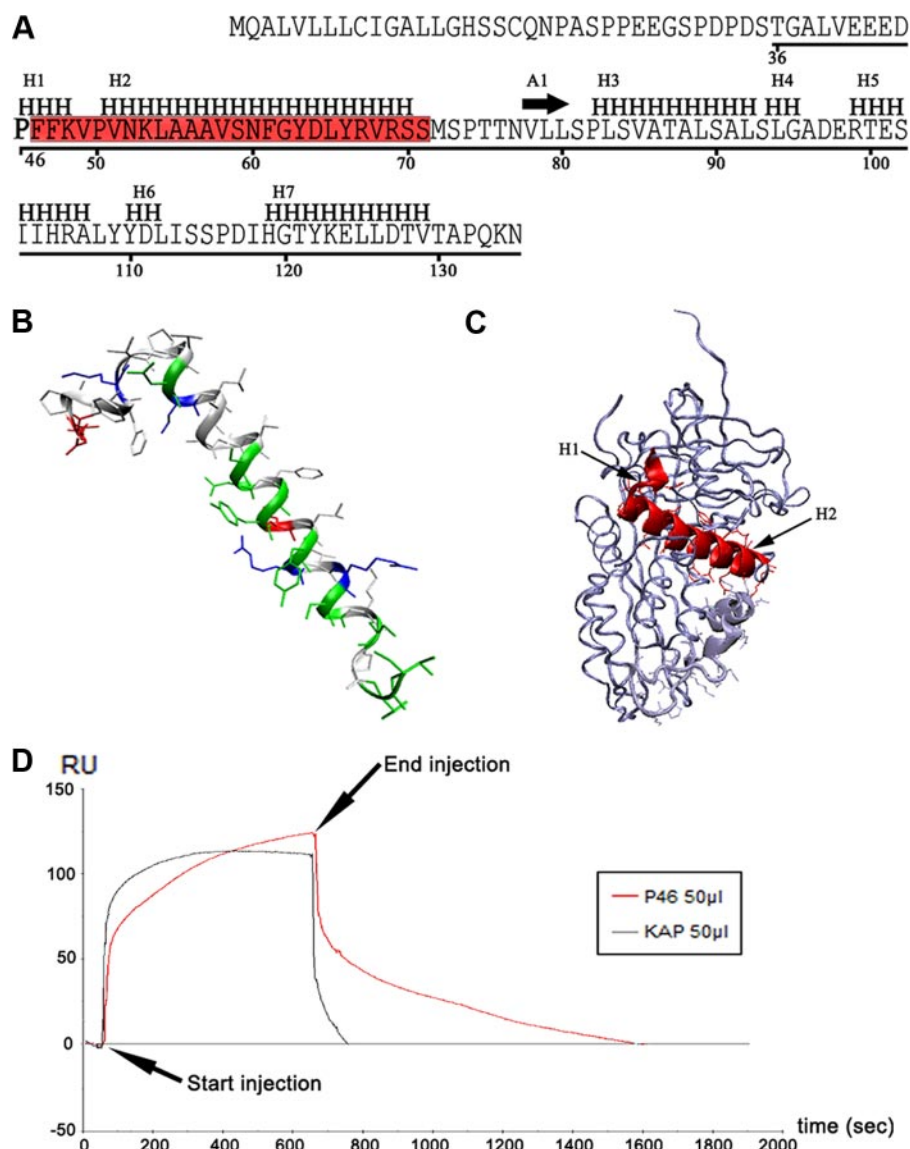


FIGURE 3. Characterizing the 25-mer peptide that specifically interacts with LR. A, partial sequence (aa 1–135) of human PEDF. Secondary structure is indicated by H for helix and A for beta sheet. The 25-mer region (aa 46–70), with a helix-loop-helix is shown in red. This 25-mer is part of a previously described 34-mer by Filleur *et al.* (25). B, secondary structure of this 25-mer. C, *in silico* analysis with VMD software shows the potential location of 25-mer P46 within the three-dimensional structure of PEDF. D, SPR assays. His-LR was immobilized on a sensor chip NTA to reach a response of between 1600 and 2000 RU. We analyzed the interaction between 25-mer and LR using a BIAcore 3000 instrument (BIAcore), according to the manufacturer's instructions. The results indicated a specific interaction between LR and 25-mer. We used peptide KAP3.1 as a negative control.

plates in complete MEB2 medium (Promocell). The next day the cells were serum-starved for 14 h by incubation in 0.2% serum MEB2 without growth factors. We then incubated cells with PEDF (40 ng/ml), P46 (200 nM), or KAP3.1 (200 nM) in the presence or absence of bFGF (20 ng/ml) and VEGF (20 ng/ml) for 24 h. We rinsed cells with PBS (pH 7.4) for 5 min twice, fixed them with 4% paraformaldehyde, and stained them according to the manufacturer's instructions. We stained cell nuclei with DAPI. We assessed the percentage of TUNEL-stained cells by fluorescence microscopy, examining four random views/sample. We repeated the experiments three times.

Wound Healing Assay—We plated HuBMECs into 12-well plates at 50,000 cells/cm² and grew them until confluent. We created a wound using a pipette cone. We then washed cells

once with culture medium and left them in Dulbecco's modified Eagle's medium supplemented with 0.5% FBS and 20 ng/ml bFGF. We monitored the wounded areas over 24 h and took micrographs every 4 h.

siRNA-mediated LR Knockdown Experiment—We seeded HuBMECs in 6-well dishes at 1×10^5 cells/well 1 day before transfection. We used four siRNA oligonucleotides (Genecust, Ivry, France) to target the human LR gene, either individually or in combination: LR-100 (5'-GGAACAGUACAUCUAUAAATT-3'/5'-UUUAUAGAUGUACUGUCCAT-3'), LR-211 (5'-UGCUGAUGUCAGUGUUAUATT-3'/5'-UAUAAACACUGACACAGCAGG-3'), LR-402 (5'-CGGAGGCAUCUUAUGUUAATT-3'/5'-UUAACAUAAGAUGCCUCCGTG-3'), and LR-612 (5'-CAGAGAUCUGAAGAGAUUTT-3'/5'-AAUCUCUUCAGGAUCUCUGTT-3').

We used scrambled siRNA (5'-UUCUCCGAACGUGUCACGUTT-3'/5'-ACGUGACACGUUCGAGAATT-3') as a negative control. The siRNA pool of the four sequences gave the best knockdown result (data not shown), and we used this in all subsequent experiments. We transfected cells with MATRA-si (IBA) 24 h later, according to the manufacturer's protocol. We analyzed silencing efficiency by immunoblotting with anti-LR antibody (H-141; Santa Cruz). We assayed active caspase-3 levels by using anti-active caspase-3 antibody (CPP32; R & D System) in a

Western blot. We repeated the experiments twice.

Statistical Analysis—We analyzed quantitative data using Fisher post hoc tests for repeated measures and Student's unpaired *t* tests. The data shown are the means \pm S.E. We considered *p* values <0.05 to be statistically significant and have marked them with asterisks.

RESULTS

Identification of 37/67-kDa LR as a PEDF Partner by the Y2H System—Considering the widespread tissue expression and distinct biological functions of PEDF, we assumed that this peptide would have a series of partners. To investigate this further, we adopted a Y2H approach, screening a human skeletal muscle cDNA library using full-length PEDF (aa 2–418) as bait. We

screened the clones grown on high stringency selected medium (SD/−Ade/−His/−Leu/−Trp/X-α-Gal). We isolated and sequenced plasmids from the clones that expressed proteins potentially interacting with GAL4-BD-PEDF. We then matched the sequences from these clones with the GenBankTM data base. Sequence analysis revealed that several of these clones encode plasma membrane proteins or potential PEDF receptors, such as PNPLA2 and 37/67-kDa LR. During our study, Becerra and co-workers (26) identified PNPLA2 as a PEDF receptor, one with potent phospholipase A₂ activity that liberates fatty acids. We therefore decided to focus on the second plasma membrane protein: the LR. 67LR is a non-integrin laminin receptor, which possesses similar heparan sulfate proteoglycan binding activity to PEDF (15, 46). It is located in the cell membrane and results from the maturation of a 37-kDa precursor, previously known as P40 or 37LRP (laminin receptor precursor) (47). 67LR plays an important role in cell proliferation and migration, angiogenesis, and tumor metastasis (39, 48). Alignment and comparison with the GenBankTM data base showed that the clones interacting with full-length PEDF contained only the 67LR extracellular domain (Fig. 1B, LRec, aa 96–295, accession number NM_002295.4). We wished to know whether the entire LR would interact with PEDF in the Y2H system, and if so, which PEDF domains would mediate the interaction.

Identification of a 37/67-kDa LR-interacting Domain on PEDF—Surprisingly, PEDF did not interact with full-length 67LR in the Y2H system (Fig. 1B). This may be due to aberrant protein folding or membrane docking caused by the presence of the transmembrane domain in the full-length LR. We performed immunofluorescence in the yeast co-transformed by the plasmids GAL4-BD-PEDF and GAL4-AD-LR using anti-GAL4-BD and anti-GAL4-AD antibodies. The results showed that the two antibodies stained the nucleus (supplemental Fig. S1), thus excluding the membrane docking hypothesis. Western blot analysis of protein expression with antibody anti-GAL4-AD detected a smaller than expected band in the yeast harboring the full-length GAL4-AD-LR plasmid (17 kDa instead of 50 kDa; supplemental Fig. S1). Furthermore we detected a 29-kDa band using anti-LR antibody. These results suggest that a protease digests the fusion protein GAL4-AD-LR, thereby separating GAL4-AD from LR. This could explain the absence of interaction between full-length LR with PEDF. Digestion of fusion protein could be linked to protein misfolding, which exposes the potential protease recognition site. To identify the LR-interacting domain on PEDF, we generated nested mutated PEDF fragments from N and C termini by PCR and linked these fragments to GAL4-BD of the vector pGBKT7 (Fig. 1A). We co-transfected these constructs with LRec (aa 96–295) linked to GAL4-AD of pGADT7 vector into yeast. The Y2H results revealed a PEDF region in N-terminal (aa 44–77) that interacts with LRec. This domain is also known as an anti-angiogenic peptide: the 34-mer peptide (25).

Characterization of PEDF-interacting Domain on LR—We generated different fragments from the extracellular domain of the LR and linked them to GAL4-AD of pGADT7 vector. These constructions were co-transfected with the full-length PEDF constructions or 34-mer PEDF peptide (aa 44–77) as described

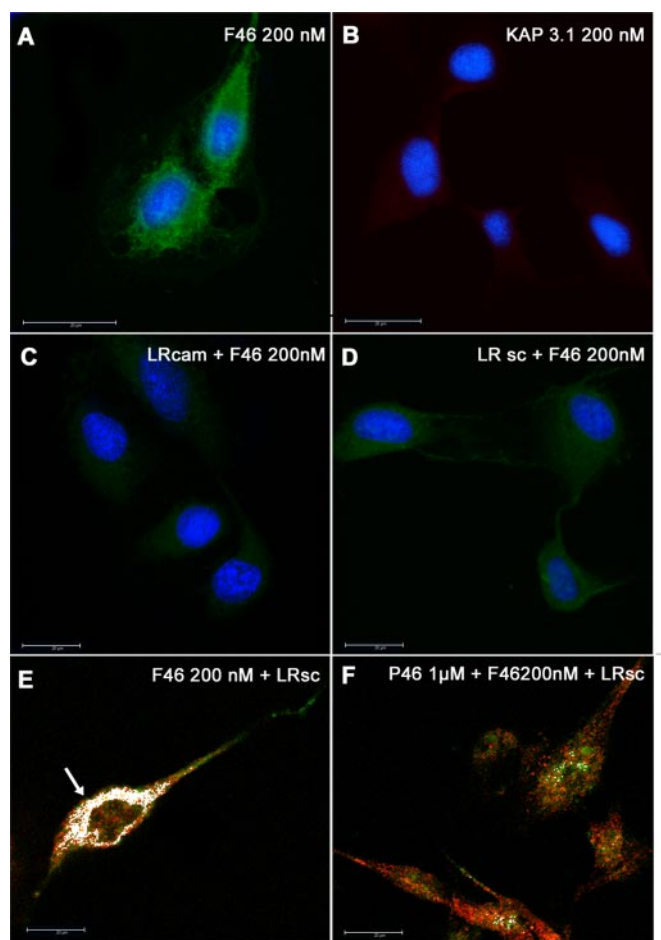


FIGURE 4. 25-mer peptide F46 binds HuBMECs. A, Fluorescent-P46 (F46) binding to HuBMECs. We incubated HuBMECs with 200 nM F46 for 60 min at 4 °C. We used DAPI (blue) to label nuclei. B, rhodamin-labeled control peptide KAP3.1 (200 nM) did not bind to HuBMECs under the same condition as A. C, F46 binding to HuBMECs was inhibited when cells were preincubated with polyclonal 67LR antibody (ab711; Abcam). D, F46 binding to HuBMECs was decreased when cells were preincubated with monoclonal 67LR antibody (H-141; Santa Cruz). E, co-localization (white) of F46 and LR on the surface of the HuBMECs. We incubated F46 with cells, as described for A, and then incubated the cells with anti-67LR antibody (H-141; Santa Cruz) to label LR. White (arrow) demonstrates the co-localization of intense green staining (F46) and red staining (67LR). F, F46 binds specifically to HuBMEC membranes. We performed experiments as detailed for E, except for adding excess non-fluorescent P46 to the cells in the binding buffer. F46 staining (green) was barely detectable. Bar, 20 μ m.

above. We showed that the PEDF-interacting domain on 67LR was restricted to fragment aa 120–210 (Fig. 1B, construction L4B). Sequences aa 120–135 and 200–210 seem essential for the interaction between PEDF and LR, because deleting these regions abolished the interaction (Fig. 1B, construction L3). However, in association with the fragments aa 157–180, 120–156, and 181–210 seem to be independently sufficient for an interaction between LR and the PEDF peptide, although the interaction with full-length PEDF seems to be diminished. Indeed, both aa 120–180 (Fig. 1B, PGR construct) and 157–210 (Fig. 1B, PGF construct) interacted with PEDF or 34-mer, unlike fragment aa 157–180 (Fig. 1B, LPG construct). LPG peptide refers to the palindromic G peptide (aa 161–179) known to interact with laminin 1 and PrP prion protein (46). Although this peptide is not able to bind PEDF alone, deleting it (Fig. 1B, Δ LPG) reduced the interaction between LR and full-length

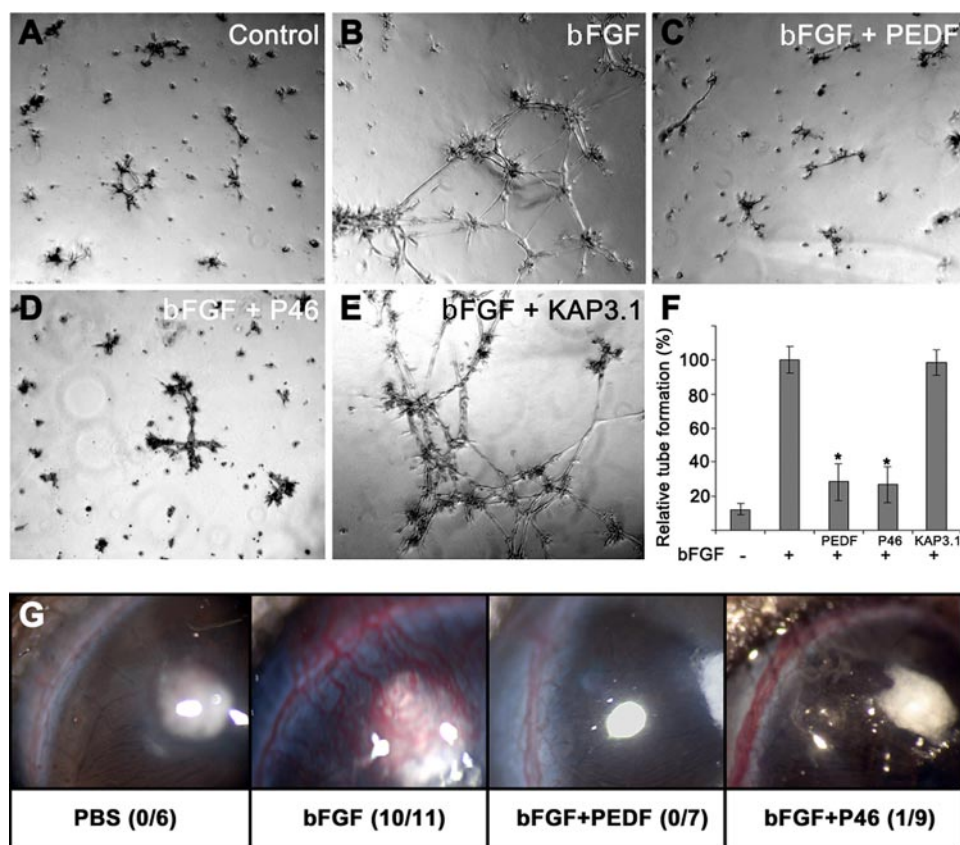


FIGURE 5. 25-mer peptide P46 inhibits bFGF-induced angiogenesis on Matrigel. We seeded HuBMECs into 24-well plates coated with Matrigel and examined tube-like structure formation by phase contrast microscopy 24 h later. *A*, control: no factors in medium. *B*, we observed tube-like structure formation after 24 h of incubation with bFGF (20 ng/ml). *C*, PEDF (40 ng/ml) inhibits bFGF-induced tube-like structure formation. *D*, peptide P46 (200 nM) inhibits tube-like structure formation, just like PEDF. *E*, control peptide KAP3.1 (200 nM) does not inhibit tube-like structure formation. *F*, graphic representation of bFGF-induced tube-like structure formation in the presence of PEDF, P46, and KAP3.1, respectively. *G*, PEDF and P46 inhibit bFGF-induced angiogenesis in corneas. We show representative corneas here, indicating the number of positive corneas/total in parentheses.

PEDF and 34-mer peptide. This indicates that LPG co-operates with other LR regions for full PEDF interaction.

PEDF and LR Co-localize in Living Cells—Because full-length LR does not interact with PEDF in the Y2H system, we co-transfected COS7 cells with HA-tagged full-length PEDF (HA-PEDF) and Myc-tagged LR (Myc-LR) using a cytomegalovirus promoter to examine potential interaction between the full-length LR and PEDF in living cells. We checked PEDF and LR expression by Western blot (Fig. 2*E*) with anti-HA and anti-Myc antibodies, respectively. As shown in Fig. 2*E*, both HA-PEDF and Myc-LR were readily expressed and detected by Western blot as 55- and 40-kDa proteins. We observed the co-localization of Myc-LR and HA-PEDF on immunofluorescence labeling in the co-transfected cells (Fig. 2, *A–C*). In addition, analysis of the confocal microscopy results also indicated that HA-PEDF and Myc-LR co-localize with a strong signal at the cell periphery (Fig. 2*D*). This co-localization suggests potential interaction of PEDF and LR at the plasma membrane of living cells.

To confirm the PEDF and LR interaction, we performed a co-immunoprecipitation experiment (Fig. 2*H*). We mixed full-length LR proteins, produced in *E. coli*, with full-length PEDF from insect Sf9 cells. Then we added either anti-PEDF or anti-LR antibody to the protein mixture, using IgG antibody as

a control. Precipitate analysis indicated that full-length PEDF co-immunoprecipitated with full-length LR (Fig. 2*H*, lanes 2 and 3) when anti-PEDF was used, indicating a direct interaction between PEDF and LR. The co-immunoprecipitation experiment with anti-LR antibodies failed to co-immunoprecipitate LR and PEDF. This could be due to the fact that anti-LR antibody recognizes a region that overlaps with the PEDF binding site on LR. To overcome this possibility, we performed a His tag pulldown assay, using His-tagged full-length LR and then His-tagged LR extracellular domain (LR90). We found that PEDF was pulled down with Ni-NTA beads when the binding reactions included His-tagged LR or His-tagged LR90 (Fig. 2*G*). We further confirmed this PEDF-LR interaction by surface plasmon resonance assay (Fig. 2*I*). Fig. 2*I* shows PEDF binding to His-tagged LR and His-tagged LR90 on the Ni²⁺-NTA surface. The overlay plot shows that the signals for PEDF binding to LR and LR90 were similar, reaching 370 RU. The following dissociation phase is slow, requiring more than 1 h to return to initial levels. PEDF did not bind to the Ni²⁺-NTA surface in the absence of LR (supplemental Fig. S2).

25-mer PEDF Peptide Binds Specifically to Cell Membranes—Previous research has indicated that PEDF binds specifically to at least two cell membrane receptors, one 80-kDa receptor and one 60-kDa receptor (21–24). The 80-kDa receptor could be the PNPLA2 (26). We propose that the 60-kDa receptor could be LR. Having demonstrated the interaction between PEDF and LR and identified a specific PEDF domain, we then investigated the biological functions of this domain. According to previous studies, the 34-mer peptide exhibits anti-angiogenic activity (25), and we wondered whether a smaller fragment could elicit the same effects. For this purpose, we used protein structure software to analyze the 34-mer (aa 44–77) to help design and synthesize a 25-mer (aa 46–70, designated as P46) with a helix-loop-helix structure (Fig. 3, *A* and *B*). This peptide is located on the surface of the three-dimensional structure of PEDF (Fig. 3*C*). We used SPR assays to evaluate the potential interaction between P46 and LR (Fig. 3*D*). Our results show that P46 interacts specifically with LR in an SPR assay. An overlay plot shows that the signal for P46-LR binding reached 45 RU and that the following dissociation phase was slow. More than 10 min were needed to return to initial levels, compared with the control peptide, which dissociated immediately. P46 did not bind to the Ni²⁺-NTA surface in the absence of LR (supplemental Fig. S2).

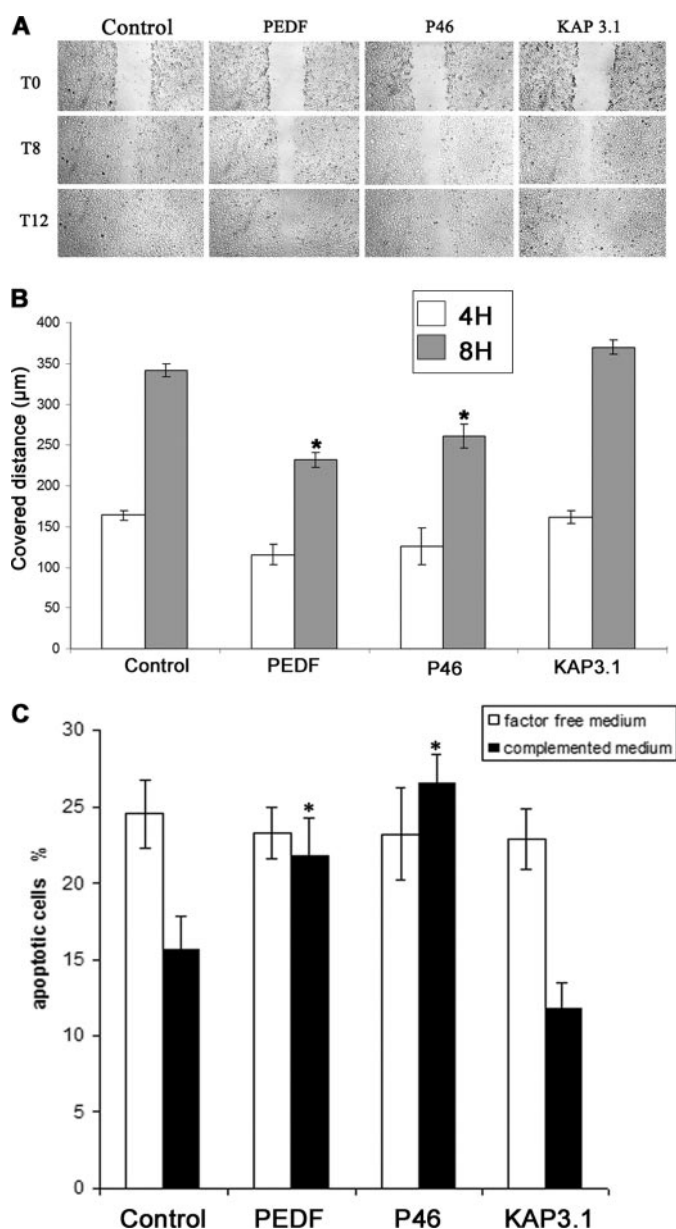


FIGURE 6. PEDF and P46 peptide decrease cell motility in wound healing assays and promote apoptosis in endothelial cells. *A*, representative pictures of wound healing experiments. PEDF or the peptides used are shown at the top of the picture, and time is marked on the left. *B*, cell migration in the presence of PEDF, P46, and KAP3.1, respectively, at 4 and 8 h. PEDF and P46 decrease cell migration. *C*, apoptotic cells in different conditions. We starved HuBMECs in factor-free 0.2% FBS MEB2 overnight and incubated them in a starved medium with or without bFGF/VEGF growth factors (20 ng/ml each) and PEDF (40 ng/ml), P46 (200 nM), P326 (200 nM), and KAP3.1 (200 nM) for 24 h. bFGF/VEGF protects cells from apoptosis under starvation conditions. We counted the percentage of TUNEL-labeled cells by fluorescence microscopy, examining four random views/sample. We repeated the experiment three times.

We verified that this peptide can bind LR on cell membranes. We incubated fluorescent P46 peptide (F46) with HuBMECs at 4 °C for 60 min and observed a strong signal (Fig. 4*A*). Our control did not show binding to HuBMECs (Fig. 4*B*). Interestingly, HuBMEC membrane binding by F46 was abolished when cells were blocked by anti-67LR polyclonal antibody ab711 (Abcam) (Fig. 4*C*), which also inhibits laminin1 signaling (13). Binding was also diminished when we used anti-LR monoclonal

antibody H-141 (Santa Cruz) (Fig. 4*D*). In addition, confocal microscopy analysis showed that F46 fluorescence co-localizes with LR revealed by anti-LR. Furthermore, this co-localization was abolished when excess unlabeled P46 was added at the same time (Fig. 4, *E* and *F*). These results indicate a specific P46-LR interaction.

25-mer Peptide P46 Shows the Same Anti-angiogenic Activity as PEDF—We know that PEDF has anti-angiogenic properties *in vitro* and *in vivo* (3–6, 25). We performed a Matrigel angiogenesis assay *in vitro* in HuBMECs to examine whether peptide P46 also has these properties. Endothelial cells form tube-like networks when grown on Matrigel using a medium containing 0.2% FBS and bFGF (20 ng/ml) for 24–48 h (Fig. 5). Our results show that P46 inhibits bFGF-induced tube-like network formation in the same way as full-length PEDF (40 ng/ml), whereas control peptide KAP3.1 (200 nM) has no effect (Fig. 5, *C–E*). We examined the effects of the peptide on angiogenesis in corneal tissue *ex vivo*, where again our results show that P46 inhibits angiogenesis as efficiently as PEDF (Fig. 5*G*).

Like PEDF, P46 Peptide Inhibits Cell Migration and Has Pro-apoptotic Activities—Wound healing assays demonstrated that, like PEDF, P46 decreases cell migration (Fig. 6, *A* and *B*). It is well established that PEDF has a pro-apoptotic effect on proliferative ECs (32). We then investigated whether P46 inhibits bFGF-induced vessel-like formation through pro-apoptotic activity. We detected apoptosis by TUNEL assays and active caspase-3 assays in the presence or absence of both VEGF (20 ng/ml) and bFGF (20 ng/ml). In the medium with 0.2% FBS and no growth factors, the percentage of TUNEL-positive cells was about 20–25% (Fig. 6*C*). We observed no significant difference between control, KAP 3.1, PEDF, and P46 treatment groups. Growth factors offer some protection to the control and KAP3.1 treated groups, reducing the percentage of TUNEL-positive cells to 12–15% in the control and in the KAP3.1-treated groups. With P46 and PEDF, however, this protective effect was lost; TUNEL-positive cells reached 28% in P46 treated cells and 23% in PEDF. To further confirm this pro-apoptotic effect, caspase-3 activation was followed by Western blots on protein extracts from cells treated for 0.5, 1, 3, and 6 h with PEDF and P46 (100 nM) (Fig. 7). We observed increased active caspase-3 production during the PEDF and P46 treatments (Fig. 7, *A*, *C*, and *D*). Interestingly, caspase activation was abolished when LR expression was blocked by siRNA inhibition. This underlines the link between PEDF treatment, PEDF-LR interaction, and the increase in apoptosis (Fig. 7).

DISCUSSION

Angiogenesis is important in physiological events such as embryonic development, but it is also implicated in pathological situations, such as cancer (49–51). Solid tumors need new vessels to grow, so selectively preventing angiogenesis has become a promising approach in anti-cancer therapy. PEDF, a natural peptide, powerfully inhibits angiogenesis *in vitro* and *in vivo* (see reviews in Refs. 3–6). Our results provide a molecular basis for this anti-angiogenic activity.

For 10 years, several groups have provided evidence suggesting that PEDF receptors exist in the plasma membranes of dif-

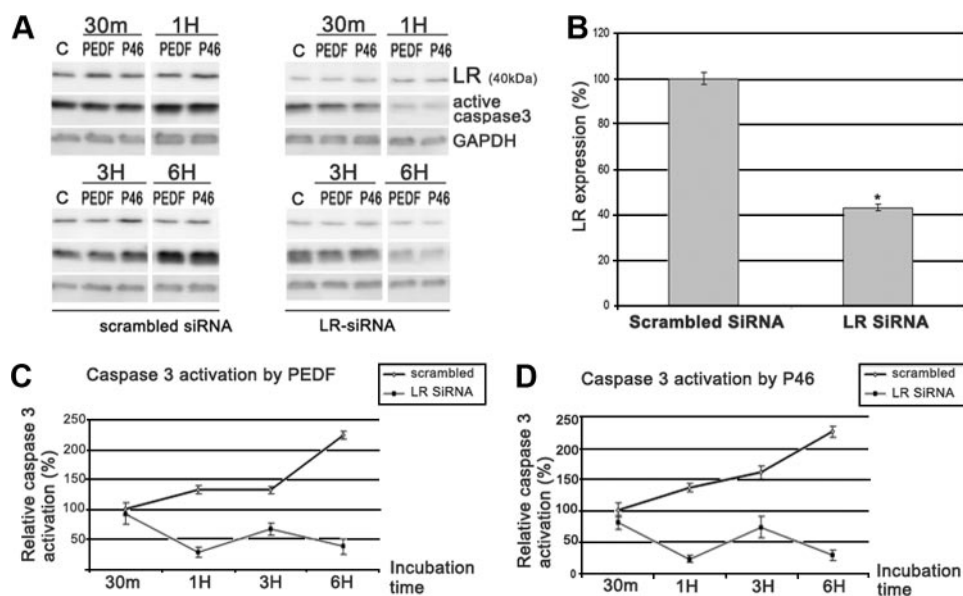


FIGURE 7. PEDF and peptides promote apoptosis by regulating caspase-3 activity. A, PEDF and P46 increase caspase-3 activation. We transfected HuBMECs with either LR siRNA or scrambled siRNA. After 48 h, we treated cells with PEDF (40 ng/ml) or P46 (200 nM) for 30 min, 1 h, 3 h, or 6 h. We analyzed lysates by immunoblotting, using anti-LR, anti-active caspase-3, and anti-glyceraldehyde-3-phosphate dehydrogenase antibodies. We have shown a representative Western blot. B, reduced LR protein expression in LR siRNA-treated HuBMECs. We measured the relative 67LR expression and found a 60% decrease in LR protein in the LR siRNA-treated cells compared with the scrambled siRNA-treated cells. C and D, relative active caspase-3 levels. Graphs show the relative active caspase-3 level (compared with control cells) in the cells treated with LR or scrambled siRNA after 30 min, 1 h, 3 h, and 6 h of incubation with PEDF (C) or P46 (D) at 37 °C. Note the reduced active caspase-3 production in the siRNA-treated cells compared with the control cells in the presence of PEDF or P46. We repeated the experiment once.

ferent cell types, distinct receptors to elicit divergent signals. At least two receptors have been proposed by earlier work: one of 60 kDa in ECs and another of 80 kDa in neuronal cells (21–24). Recently, PNPLA2 has been identified as a PEDF receptor (26). With its phospholipase activity, PNPLA2 could be the 80-kDa receptor identified in neuronal cells. PEDF could exert its neuroprotective activity and regulate fatty acid/lipid metabolism in ocular and liver tissue through this receptor (26, 52).

We have identified a second PEDF receptor: the LR. This may be related to the 60-kDa receptor previously reported in ECs (24). It has been suggested that the 67-kDa laminin receptor (67LR) consists of two 37LRP (37-kDa laminin receptor precursor) polypeptide chains and that the 67LR mature form involves 37LRP acylation (53). The relationship between 37LRP and 67LR remains poorly understood. In this study, we have identified LR as a PEDF receptor for the first time. We have shown that entire PEDF interacts with the extracellular region of 37LRP/67LR, but not with entire 37LRP/67LR, in Y2H experiments (Fig. 1). Other approaches, such as immunoprecipitation, His tag pulldown and SPR assays, indicate that entire PEDF can interact with entire 37LRP/67LR (Fig. 2). This difference in results could be related to a transmembrane domain in full-length LR causing aberrant protein folding or membrane docking. Immunofluorescence shows that both PEDF and fluorescent 25-mer PEDF peptide co-localize with LR on plasma membranes, suggesting the potential interaction site of PEDF with LR (Figs. 2 and 4). We further identified a 25-mer peptide, derived from PEDF, as a major PEDF-LR interaction region. 25-mer can interact with LR, bind to cell membranes, induce EC apoptosis, inhibit EC migration, and block angiogenesis *in*

vitro and *ex vivo*, just like PEDF (Figs. 3–7). Several pathways have been suggested to explain the anti-angiogenic activity of PEDF, such as inducing EC death by activating the Fas/FasL death pathway (31). However, PEDF still inhibits neovascularization in mice lacking either Fas or FasL (54), implying that either other pathways are involved or that PEDF does not use Fas-FasL interactions to inhibit retinal neovascularization. Following this hypothesis, other groups have reported that MAPK JNK and p38 influence EC apoptosis by modulating c-FLIP or caspase activity (32, 33). Furthermore, Cai *et al.* (34) reported that PEDF inhibits VEGF-induced angiogenesis in bovine retinal microvascular ECs by enhancing γ -secretase-dependent cleavage of the C terminus of VEGF receptor-1, which consequently inhibits VEGF receptor-2-induced angiogenesis. We have shown that knockdown LR in endothelial cells decrease the

active caspase-3 content (Fig. 7). Our data indicate that the anti-angiogenic activity of PEDF is at least partially mediated by binding LR. The main question is this: Is PEDF-LR binding the major signaling event that inhibits angiogenesis? Further experiments are needed to clarify the effects of PEDF-LR interaction, with regard to other reported pathways used by PEDF to mediate anti-angiogenesis and apoptosis in ECs.

67LR is expressed in tumoral (55), muscular (56), neuronal (57), epithelial (58), and endothelial (59) cells. Indeed, both PEDF and 67LR are involved in many biological processes, such as migration (60, 61), adhesion (62, 63), and proliferation (64) in many cell types. Like PEDF, 67LR is also implicated in retinal neuronal differentiation and vascular development (65–67). In mice, proliferating ECs express 67LR at high levels during retinal neovascularization. Both 67LR mRNA and protein expression show a characteristic biphasic expression pattern at key stages of retinal vascular development: P1 (postnatal day 1, correlates with superficial vascular plexus formation) and P7 (correlates with deep vascular plexus formation). Conversely, 67LR expression decreases when angiogenic activity is lower (65). In addition, 37LRP expression correlates well with the biological aggressiveness of cancer cells. Decreased expression of 37LRP by antisense RNA gives rise to low tumorigenicity, caused by the diminished tumor angiogenesis of murine lung cancer (68). In this study, we used Y2H method to identify a PEDF region (aa 44–77, previously described as 34-mer (25)) that interacts with aa 120–210 of the 67LR extracellular domain, which included the palindromic 67LR G peptide (aa 161–179), known to interact with laminin 1 (57). Interestingly, 67LR G peptide by itself

did not interact with either PEDF or 34-mer in Y2H experiments. Flanking regions, either the N-terminal region (aa 120–156) or the C-terminal region (aa 181–210), are independently required, but not sufficient, for full interaction; their own interaction with PEDF was reduced when we deleted G peptide from 67LRec (Fig. 1B). The 34-mer peptide mediates some aspects of anti-angiogenesis (25). Our major finding is that a 25-mer peptide, containing a helix-loop-helix structure, mediates PEDF binding to LR (Figs. 3 and 4) and that this peptide, like PEDF, inhibits angiogenesis *in vitro* and *ex vivo* (Fig. 5). This peptide seems to inhibit angiogenesis by altering cell migration and increasing apoptosis, as demonstrated by wound healing assays, TUNEL labeling (Fig. 6) and caspase-3 activation studies (Fig. 7). P46, therefore, could potentially block tumor neovascularization without interfering with other PEDF effects. PEDF only targets new vessel growth, sparing pre-existing vasculature, which makes it an appealing candidate for blocking tumor angiogenesis (3–6, 69). Thus, the 25-mer has a potential role in treating cancer and retinopathies by inhibiting angiogenesis.

Cell interaction with the laminin component of basement membranes is important for normal cell function. LR not only acts as a receptor for laminin but also binds viruses (36–38) and the prion protein (35). In fact, 37LRP/67LR binds prion proteins (PrP). Furthermore, 37LRP/67LR binds heparan sulfate proteoglycan, which might be necessary for receptor/ligand interaction (46). The 25-mer PEDF-interacting domain of 67LR includes peptide G, between residues 161–179, a domain necessary for laminin and PrP binding (70). Fluorescent 25-mer peptide (F46) could not bind to endothelial cells in the presence of anti-67LR antibody (Fig. 4), an antibody already known to inhibit laminin1 binding to its 67LR receptor. It will be interesting to investigate whether 25-mer peptide interferes with these interactions and to explore its possible therapeutic properties.

In conclusion, we have demonstrated that: 1) LR is a novel PEDF receptor; 2) the LR-interacting region on PEDF is restricted to a 25-mer P46 (residue 46–70); 3) the PEDF-interacting domain on LR is located between aa 120 and 210, which includes the laminin1 and PrP-binding domains of LR; and 4) this 25-mer P46, which binds specifically to EC membranes, inhibits bFGF-induced angiogenesis *in vitro* and *ex vivo* by inducing apoptosis and reducing cell migration. These results reveal a new signaling pathway for the anti-angiogenic activities of PEDF. Modulating LR activity could provide an attractive option for treating angiogenesis-dependent disease, such as metastatic cancer.

Acknowledgments—We thank Dr. D. Paulin, M. Andreani, A. Torriglia, Dr. C. Piesse, and laboratory members for fruitful discussions and suggestions; Dr. M. K. Zhang for help with our corneal angiogenesis experiments; and Dr. S. Thibaut for the generous gift of KAP3.1 peptide and for help with confocal microscopy.

REFERENCES

- Tombran-Tink, J., Chader, G. G., and Johnson, L. V. (1991) *Exp. Eye Res.* **53**, 411–414
- Tombran-Tink, J., Mazuruk, K., Rodriguez, I. R., Chung, D., Linker, T., Englander, E., and Chader, G. J. (1996) *Mol. Vis.* **2**, 11
- Bouck, N. (2002) *Trends Mol. Med.* **8**, 330–334
- Tombran-Tink, J., and Barnstable, C. J. (2003) *Nat. Rev. Neurosci.* **4**, 628–636
- Becerra, S. P. (2006) *Exp. Eye Res.* **82**, 739–740
- Ek, E. T., Dass, C. R., and Choong, P. F. (2006) *Trends Mol. Med.* **12**, 497–502
- Zhang, S. X., Wang, J. J., Gao, G., Shao, C., Mott, R., and Ma, J. X. (2006) *FASEB J.* **20**, 323–325
- Yamagishi, S., Nakamura, K., Ueda, S., Kato, S., and Imaizumi, T. (2005) *Cell Tissue Res.* **320**, 437–445
- Liu, H., Ren, J. G., Cooper, W. L., Hawkins, C. E., Cowan, M. R., and Tong, P. Y. (2004) *Proc. Natl. Acad. Sci. U. S. A.* **101**, 6605–6610
- Yamagishi, S., Inagaki, Y., Amano, S., Okamoto, T., Takeuchi, M., and Makita, Z. (2002) *Biochem. Biophys. Res. Commun.* **296**, 877–882
- Steele, F. R., Chader, G. J., Johnson, L. V., and Tombran-Tink, J. (1993) *Proc. Natl. Acad. Sci. U. S. A.* **90**, 1526–1530
- Stellmach, V., Crawford, S. E., Zhou, W., and Bouck, N. (2001) *Proc. Natl. Acad. Sci. U. S. A.* **98**, 2593–2597
- Selleri, C., Ragno, P., Ricci, P., Visconte, V., Scarpato, N., Carriero, M. V., Rotoli, B., Rossi, G., and Montuori, N. (2006) *Blood* **108**, 2476–2484
- Simonovic, M., Gettins, P. G., and Volz, K. (2001) *Proc. Natl. Acad. Sci. U. S. A.* **98**, 11131–11135
- Alberdi, E., Hyde, C. C., and Becerra, S. P. (1998) *Biochemistry* **37**, 10643–10652
- Yasui, N., Mori, T., Morito, D., Matsushita, O., Kourai, H., Nagata, K., and Koide, T. (2003) *Biochemistry* **42**, 3160–3167
- Becerra, S. P., Perez-Mediavilla, L. A., Weldon, J. E., Locatelli-Hoops, S., deS Senanayake, P., Notari, L., Notario, V., and Hollyfield, J. G. (2008) *J. Biol. Chem.* **283**, 33310–33320
- Meyer, C., Notari, L., and Becerra, S. P. (2002) *J. Biol. Chem.* **277**, 45400–45407
- Hosomichi, J., Yasui, N., Koide, T., Soma, K., and Morita, I. (2005) *Biochem. Biophys. Res. Commun.* **335**, 756–761
- Alberdi, E. M., Weldon, J. E., and Becerra, S. P. (2003) *BMC Biochem.* **4**, 1
- Alberdi, E., Aymerich, M. S., and Becerra, S. P. (1999) *J. Biol. Chem.* **274**, 31605–31612
- Bilak, M. M., Becerra, S. P., Vincent, A. M., Moss, B. H., Aymerich, M. S., and Kuncel, R. W. (2002) *J. Neurosci.* **22**, 9378–9386
- Aymerich, M. S., Alberdi, E. M., Martínez, A., and Becerra, S. P. (2001) *Investig. Ophthalmol. Vis. Sci.* **42**, 3287–3293
- Yamagishi, S., Inagaki, Y., Nakamura, K., Abe, R., Shimizu, T., Yoshimura, A., and Imaizumi, T. (2004) *J. Mol. Cell Cardiol.* **37**, 497–506
- Filleur, S., Volz, K., Nelius, T., Mirochnik, Y., Huang, H., Zaichuk, T. A., Aymerich, M. S., Becerra, S. P., Yap, R., Veliceasa, D., Shroff, E. H., and Volpert, O. V. (2005) *Cancer Res.* **65**, 5144–5152
- Notari, L., Baladron, V., Aroca-Aguilar, J. D., Balko, N., Heredia, R., Meyer, C., Notario, P. M., Saravanamuthu, S., Nueda, M. L., Sanchez-Sanchez, F., Escribano, J., Laborda, J., and Becerra, S. P. (2006) *J. Biol. Chem.* **281**, 38022–38037
- Duh, E. J., Yang, H. S., Suzuma, I., Miyagi, M., Youngman, E., Mori, K., Katai, M., Yan, L., Suzuma, K., West, K., Davarya, S., Tong, P., Gehlbach, P., Pearlman, J., Crabb, J. W., Aiello, L. P., Campochiaro, P. A., and Zack, D. J. (2002) *Investig. Ophthalmol. Vis. Sci.* **43**, 821–829
- Hutchings, H., Maitre-Boube, M., Tombran-Tink, J., and Plouët, J. (2002) *Biochem. Biophys. Res. Commun.* **294**, 764–769
- Kanda, S., Mochizuki, Y., Nakamura, T., Miyata, Y., Matsuyama, T., and Kanetake, H. (2005) *J. Cell Sci.* **118**, 961–970
- Doll, J. A., Stellmach, V. M., Bouck, N. P., Bergh, A. R., Lee, C., Abramson, L. P., Cornwell, M. L., Pins, M. R., Borensztajn, J., and Crawford, S. E. (2003) *Nat. Med.* **9**, 774–780
- Volpert, O. V., Zaichuk, T., Zhou, W., Reiher, F., Ferguson, T. A., Stuart, P. M., Amin, M., and Bouck, N. P. (2002) *Nat. Med.* **8**, 349–357
- Zaichuk, T. A., Shroff, E. H., Emmanuel, R., Filleur, S., Nelius, T., Volpert, O. V. (2004) *J. Exp. Med.* **199**, 1513–1522
- Chen, L., Zhang, S. S., Barnstable, C. J., and Tombran-Tink, J. (2006) *Biochem. Biophys. Res. Commun.* **348**, 1288–1295
- Cai, J., Jiang, W. G., Grant, M. B., and Boulton, M. (2006) *J. Biol. Chem.* **281**, 3604–3613

35. Gauczynski, S., Peyrin, J. M., Haïk, S., Leucht, C., Hundt, C., Rieger, R., Krasemann, S., Deslys, J. P., Dormont, D., Lasmézas, C. I., and Weiss, S. *EMBO J.* **20**, 5863–5875
36. Wang, K. S., Kuhn, R. J., Strauss, E. G., Ou, S., and Strauss, J. H. (1992) *J. Virol.* **66**, 4992–5001
37. Thepparit, C., and Smith, D. R. (2004) *J. Virol.* **78**, 12647–12656
38. Akache, B., Grimm, D., Pandey, K., Yant, S. R., Xu, H., and Kay, M. A. (2006) *J. Virol.* **80**, 9831–9836
39. Nelson, J., McFerran, N. V., Pivato, G., Chambers, E., Doherty, C., Steele, D., and Timson, D. J. (2008) *Biosci. Rep.* **28**, 33–48
40. Lee, F. J., Huang, C. F., Yu, W. L., Buu, L. M., Lin, C. Y., Huang, M. C., Moss, J., and Vaughan, M. (1997) *J. Biol. Chem.* **272**, 30998–31005
41. von der Haar, T. (2007) *PLoS ONE* **2**, e1078
42. Schweitzer, K. M., Vicart, P., Delouis, C., Paulin, D., Dräger, A. M., Langenhuijsen, M. M., Weksler, B. B. (1997) *Lab. Invest.* **76**, 25–36
43. Thibaut, S., Cavusoglu, N., De Becker, E., Zerbib, F., Bednarczyk, A., Schaeffer, C., Van Dorsselaer, A., and Bernard, B. A. (2008) *J. Invest. Dermatol.* **129**, 449–459
44. Franco, C. A., Mericskay, M., Parlakian, A., Gary-Bobo, G., Gao-Li, J., Paulin, D., Gustafsson, E., and Li, Z. (2008) *Dev. Cell* **15**, 448–461
45. Kenyon, B. M., Voest, E. E., Chen, C. C., Flynn, E., Folkman, J., and D'Amato, R. J. (1996) *Investig. Ophthalmol. Vis. Sci.* **37**, 1625–1632
46. Hundt, C., Peyrin, J. M., Haïk, S., Gauczynski, S., Leucht, C., Rieger, R., Riley, M. L., Deslys, J. P., Dormont, D., Lasmézas, C. I., and Weiss, S. (2001) *EMBO J.* **20**, 5876–5886
47. Ardini, E., Pesole, G., Tagliabue, E., Magnifico, A., Castronovo, V., Sobel, M. E., Colnaghi, M. I., and Ménard, S. (1998) *Mol. Biol. Evol.* **15**, 1017–1025
48. Ardini, E., Sporchia, B., Pollegioni, L., Modugno, M., Ghirelli, C., Castiglioni, F., Tagliabue, E., and Ménard, S. (2002) *Cancer Res.* **62**, 1321–1325
49. Hanahan, D., and Folkman, J. (1996) *Cell* **86**, 353–364
50. Risau, W. (1997) *Nature* **386**, 671–674
51. Carmeliet, P. (2005) *Nature* **438**, 932–936
52. Chung, C., Doll, J. A., Gattu, A. K., Shugrue, C., Cornwell, M., Fitch, P., and Crawford S. E. (2008) *J. Hepatol.* **48**, 471–478
53. Butò, S., Tagliabue, E., Ardini, E., Magnifico, A., Ghirelli, C., Van den Brùle, F., Castronovo, V., Colnaghi, M. I., Sobel, M. E., and Ménard, S. (1998) *J. Cell Biochem.* **69**, 244–251
54. Berreiro, R., Schadlu, R., Herndon, J., Kaplan, H. J., and Ferguson, T. A. (2003) *Investig. Ophthalmol. Vis. Sci.* **44**, 1282–1286
55. Givant-Horwitz, V., Davidson, B., and Reich, R. (2004) *Cancer Res.* **64**, 3572–3579
56. Lesot, H., Kuhl, U., and Von den Mark, K. (1983) *EMBO J.* **2**, 861–865
57. Kleinman, H. K., Ogle, R. C., Cannon, F. B., Little, C. D., Sweeney, T. M., and Luckenbill-Edds, L. (1988) *Proc. Natl. Acad. Sci. U. S. A.* **85**, 1282–1286
58. Terranova, V. P., Aumailley, M., Sultan, L. H., Martin, G. R., and Kleinman, H. K. (1986) *J. Cell Physiol.* **127**, 473–479
59. Stitt, A. W., McKenna, D., Simpson, D. A. C., Gardiner, T. A., Harriott, P., Archer, D. B., and Nelson, J. (1998) *Am. J. Pathol.* **152**, 1359–1365
60. Dawson, D. W., Volpert, O. V., Gillis, P., Crawford, S. E., Xu, H., Benedict,., and Bouck, N. P. (1999) *Science* **285**, 245–248
61. Scott, W. N., McFerran, N. V., Harriott, P., Walker, B., and Nelson, J. (2000) *Biochim. Biophys. Acta* **1481**, 25–36
62. Ek, E. T., Dass, C. R., Contreras, K. G., and Choong, P. F. (2007) *J. Orthop. Res.* **25**, 1671–1680
63. Wewer, U. M., Taraboletti, G., Sobel, M. E., Albrechtsen, R., and Liotta, L. A. (1987) *Cancer Res.* **47**, 5691–5698
64. Donaldson, E. A., McKenna, D. J., McMullan, T. B., Scott, W. N., Stitt, A. W., and Nelson, J. (2000) *Mol. Cell Biol. Res. Commun.* **3**, 53–59
65. McKenna, D. J., Simpson, D. A., Feeney, S., Gardiner, T. A., Boyle, C., Nelson, J., and Stitt, A. W. (2001) *Exp. Eye Res.* **73**, 81–92
66. Behling, K. C., Surace, E. M., and Bennett, J. (2002) *Mol. Vis.* **8**, 449–454
67. Gebarowska, D., Stitt, A. W., Gardiner, T. A., Harriott, P., Greer, B., and Nelson, J. (2002) *Am. J. Pathol.* **160**, 307–313
68. Tanaka, M., Narumi, K., Isemura, M., Abe, M., Sato, Y., Abe, T., Saijo, Y., Nukiwa, T., and Satoh, K. (2000) *Cancer Lett.* **153**, 161–168
69. Sasaki, Y., Naishiro, Y., Oshima, Y., Imai, K., Nakamura, Y., and Tokino, T. (2005) *Oncogene* **24**, 5131–5136
70. Castronovo, V., Taraboletti, G., and Sobel, M. E. (1991) *J. Cell Biochem.* **266**, 20440–20446